Stability Analysis of Geotextile Reinforced Marine Causeways

Heba Koura[1], Ehab Tolba[2], and Elsayed Galal[3]

ABSTRACT

The use of geotextile tubes as retaining systems, geotechnical applications, and coastal protection in temporary and permanent structures is gaining lots of concern throughout recent decades. In the present study, computer software, ABAQUS, was used to investigate the stability of geotubes as soil retaining structure for marine causeway. Nine scenarios comprised of two geotubes lining the side of a 1:1 slope causeway were modeled to explore their effect on the causeway displacement under surcharge loads. The stability of the system was investigated by using different deformed shapes of geotubes. These deformed shapes were obtained by using different pumping pressures (0.0, 5.0, and 20.0 kPa). Moreover, the effect of tidal range was studied by defining different water depths (0.5, 1.5, and 2.5 m measured from the causeway toe). The results showed that the use of geotextile tubes subjected to pumping pressure of 0.0 and 5.0 kPa improves the deformation behavior of the causeway with water depths of 0.5 and 1.5 m. While, the deformation was aggravated with water depth of 2.5 m when using geotextile tubes subjected to pumping pressures of 0.0, 5.0, and 20.0 kPa. On the other hand, the model ceased when applying pumping pressure of 20.0 kPa with water depths of 0.50 and 1.50 m due to the failure of the upper tube. Therefore, it is recommended to use the geotextile tubes subjected to pumping pressure of 0.0 and 5.0 kPa in case of lower water depths only.
Keywords: Geotextile Tubes; Pumping Pressure; Marine Causeways; ABAQUS; Slope Stability.

1.INTRODUCTION

The application of geotextiles as a system of reinforcement has significantly advanced during the recent decades and this improved the performance of embankment structures. There are many researches recommended the use of geotextile as embankment reinforcement material (e.g., [4]; [10]; and [13]). Figure 1 shows how the geotextile tubes applied in several protection and storage works. Geotextile tube, a permeable geotextile wrap (typically woven fabrics), is considered a new trend of geotextile products that is currently used as retaining structures [7].

[1]*Civil engineer at Suez Canal authority, Port Said, Egypt, corresponding author, email: hebakoura91@gmail.com*

[2]*Professor, Faculty of Engineering, Port Said University, Port Said, Egypt, email: prof.tolba@gmail.com*

[3]*Associate professor, Faculty of Engineering, Port Said University, Port Said, Egypt, email: elsayed.galal@psu.eng.edu.eg*

This tube is hydraulically filled with a filling material (pressurized slurry or sand). The tube is provided with inlet openings on its upper surface for the attachment of a pipe that transports hydraulic fill into the tube.

High strength geotextile tubes have been successfully used worldwide to provide stability for an embankment system supported by geotextile tubes stacking on ground base foundation. Reference [11] studied the stability of geotextile tubes and migration of sand filling the tubes during wave attack. They concluded that the deformation of the tubes was a function of the filling ratio and sliding was the main failure mode, while, migration of sand within the tube did not lead to any failure. Also, they concluded that the friction was supposed to be the most important stabilizing factor and should be considered during studying the stability of the structure. The friction coefficient between elements and the friction coefficient between the elements and the foundation have considered the main governing factors that affect the development of friction. Moreover, it depends on the weight of overlapping

Figure 1: Applications of geotextile tubes in several protection and storage works.

elements that may change due to the length of contact areas and the migration of sand within the element that may vary due to the individual displacements.

Reference [3] investigated the hydraulic stability of geotextile tubes with filling percentage of 80% of sand against wave attack by executing seven large scale two dimensional physical models. He found that sliding was the significant failure mechanism for a structure constructed from stacked, 80% sand filled, geotextile tubes as the crest tube was subjected to the most severe loading. He found also that double tube crest structure was more stable than single tube crest structures.

As the deformed shape of the geotubes is governing the number and the configuration of geotubes systems used as a soil retention structure from a stability point of view, the accurate determination of the deformed shape is considered the key factor in such systems. Although the determination of the deformed shape through laboratory experiments is considered the standard and most accurate

method, they are considered tedious, expensive, labour intensive, and time-consuming. Numerical methods, on the other hand, are considered the best alternate to avoid the aforementioned obstacles. Reference [5] developed Geocops computer software as an example of numerical models which is used to solve nonlinear equation which governs the shape of the tube. This computer software used Timoshenko's method [2] to determine the deformed shape of the geotube cross section based on the unit weight of the slurry and the pumping pressure. Reference [2] presented alternate methods for calculating tube forces and shapes and the results of these methods were corresponding well with Geocops software. Reference [12] presented a scheme that can be used to determine the relationship between tube size, unit weigh of slurry, pumping pressures, and tension force. Reference [7] used ABAQUS software to model stacked geotubes through three dimensional finite element method as soil retention structure and explored their impact on embankment slope stability due to gravity and surcharge loads. He investigated four different designs during simulations in order to provide more stabilization for geotubes. These designs were: 1) using a rigid wall against the lower tube, 2) adding a geotextile blanket with the stacked tubes, 3) using equally spacing stakes against the lower tube, and 4) applying different size tubes increasing gradually in diameter from top to bottom. He concluded that the first design reduce the embankment lateral movement, but the model was unrealistic with providing a rigid wall against the lower tube. The second design couldn't be modeled by ABAQUS. Enlarged lateral displacement of the embankment was occurring during the third design, while, it marginally reduced shear stresses and plastic strains. The final design was the most stable design, but it did not achieved the target in improving the slope stability of the embankment.

The results mentioned above made it possible to come to an update in this paper. In the present work the effect of pumping pressures on the deformed shape of geotubes was investigated. In addition, the effect of stacked geotubes on the stability of the slope of a marine causeway under varying water depths due to tidal effect was studied. It is worth mentioning that the deformed shape of each geotube was determined also by using ABAQUS software.

2. METHODLOGY

The ABAQUS model (i.e., a finite element model) was used to investigate the effect of adding two geotextile tubes along a 1:1 causeway slope surface on improving its lateral displacement. The ABAQUS model was primarily used to obtain lateral displacements on a causeway subjected to varying water depths without using geotubes (reference scenarios). Then, many scenarios were performed to determine the lateral displacement when reinforcing the slope of causeway by two geotubes subjected to different pumping pressures. For sub-models of geotubes, the ABAQUS model was used to obtain the

deformed shape of the tubes due to the effect of the pumping pressure and the filling material. Then, simulations were conduced to study the influence of the deformed geotubes on improving slope stability of the causeway.

2.1. Model setup

2.1.1. Primary models

These models were done to get the deformed shapes of each tube which retains the slope surface, separately by creating a series of sub-models, each simulating a different stage of filling procedure of the tubes. The results from each of these sub-models can then be used as initial conditions for the consequent one, resulting in an integrated model describing the behavior of the structure.

Sub- model 1: shell bottom tube and rigid surface

In the first sub-model, one blank shell tube was defined as a uniform cylinder with 6.0 m long, 2.0 m diameter, and 3.0 mm wall thickness which represents an expressive segment cut out of a long tube. The tube was then retained on an analytical rigid surface representing the desired causeway near the slope toe. The model is similar to the experimental setup of Liu [6]. Approximately, square elements of dimensions of 0.12 m x 0.12 m were used for the discretization of the tube. Linear integration was applied to make the computation time shorter and nonlinear geometry option was activated during simulation. As given be [8], the shell elements were assigned as an isotropic linear elastic material with unit weight, Young's Modulus of elasticity, and Poisson's ratio of 0.75 kN/m^3, 7040.00 kN/m^2, and 0.45, respectively.

The origin point for the coordinates system was located at the toe of the slope. The x, y, and z axes were assigned horizontally perpendicular to the length of the tubes, parallel with the length of the tubes, and vertically towards the top of the structure, respectively as shown in Figure 2. These axes were symbolized as the coordinates 1, 2, and 3. Boundary conditions were set as the following: the shell tube was restrained along its vertical centerlines. These centerlines were running along the vertical planes of symmetry in z-direction. Their movements were restrained in the x and y directions. The x restraint will avoid crinkling possibility of the shell elements. The y restraint will achieve perpendicular stability to the tube during deformation process. A contact interaction was assigned during simulation between the rigid surface and tube.

Pumping pressure of 0.0, 5.0, and 20.0 kPa were used in order to obtain different deformed shapes of tubes. The additional small deformation amount was also occurring due to the effect of the own weight of the geotextile tube. The initial shapes of the single tube can be seen in Figure 2 and deformed shapes can be seen in Figure 3. The resultant deformed shape was taken as initial geometry for the lower tube in stacking configuration. The simulation results were

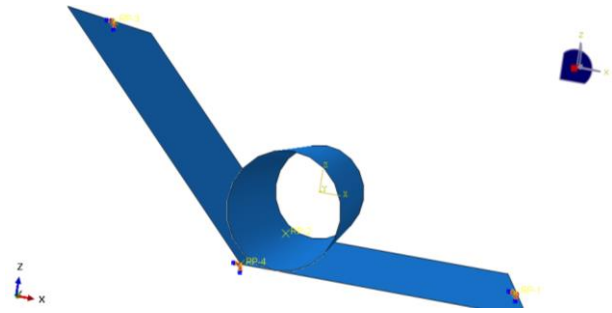concurring with the deformation behavior shown by Liu experiments [6].

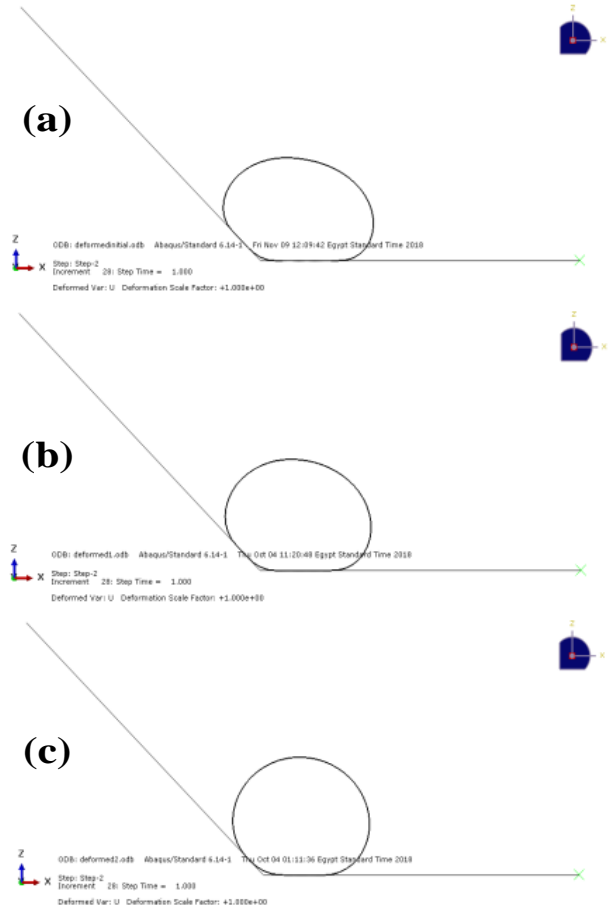**Figure 2: Sub-model 1 (initial shape of geotube resting on a rigid surface).**

(a)

(b)

(c)

Figure 3: Lower tube deformed shape subjected to pumping pressure: (a) p = 0.0 kPa, p = 5.0 kPa, and (c) p = 20.0kPa.

Sub-model 2: Rigid lower tube and shell upper tube

From the deformed shape resulted from the first sub-model, same tube with respect to size and shape was assigned. Howeverl, the lower tube was defined as an analytical rigid surface. Same analytical rigid surface as the one used in sub-model 1 was assigned for the tubes to

33

be placed on. To represent the friction between the tube and the soil slope surface, a friction coefficient of 0.50 was assigned [7].
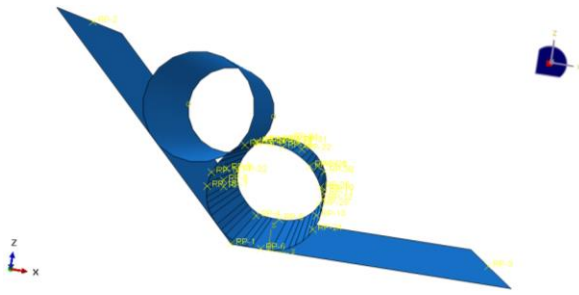

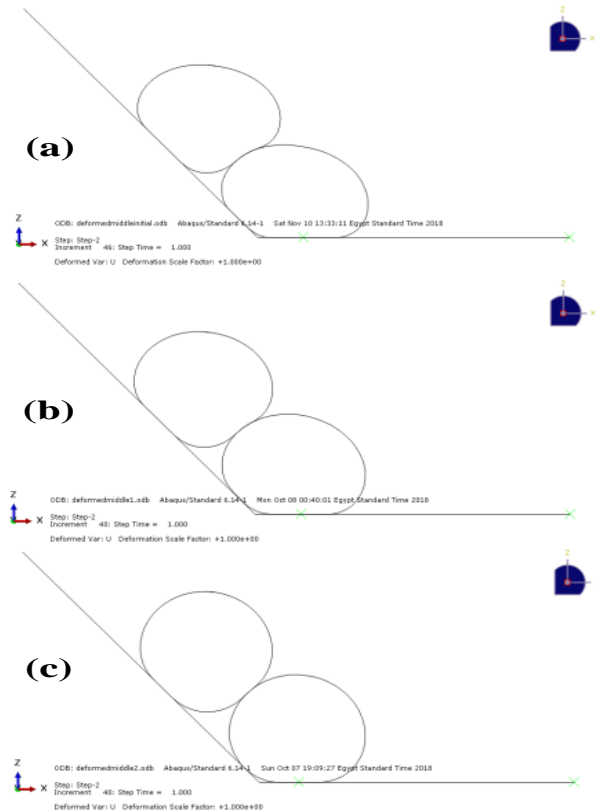**Figure 4: Sub-model 2 (initial shape of top tube).**

(a)

(b)

(c)

Figure 5: Sub-model 2 deformed shape of subjected to pumping pressure: : (a) p = 0.0 kPa, p = 5.0 kPa, and (c) p = 20.0kPa.

Also, a contact interaction with a friction coefficient of 0.30 was set between the tubes.

Figure 4 shows the model used to get the deformed shape of the upper tube. The shell tube is then loaded internally with different pumping pressures equal to 0.0, 5.0, and 20.0 kPa. The obtained deformed shapes of the upper tube were shown in Figure 5.

2.1.2. Slope stability analysis for reference scenarios

A 1:1 slope surface of a causeway with homogenous soil and without geotextile tubes was simulated by ABAQUS. The soil in the causeway was assumed to be homogenous and same soil was used as a filling material for the geotubes as shown later. The typical causeway configuration was shown in Figure 6. Cap plasticity was chosen to represent the anticipated behavior of the causeway soil. Tables 1 and 2 represent the soil parameters used in the model as defined by [9].

Table 1: Sand soil parameters used during simulation.

Elasticity	
Soil mass density (γ)	17.50 kN/ m^3
Poisson ratio (ν)	0.45
Young modulus of elasticity (E)	8500.00 kN/m^2
Plasticity	
Internal friction angle (φ)	35°
Cohesion coefficient (C)	10.0 kN/m^2
Flow stress ratio	1.00
Cap eccentricity (R)	0.45

Table 2: Cap hardening parameters for sand soil.

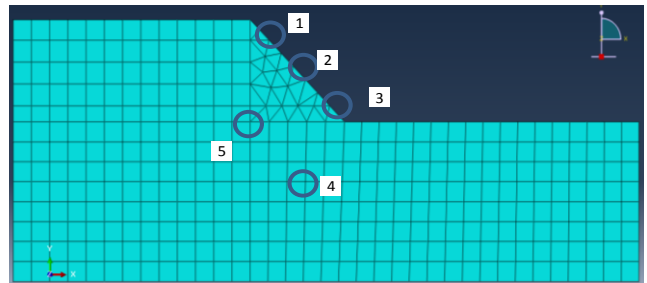|	Stress (Pa)	Volumetric plastic strain
1	8200	0.000
2	38900	0.009
3	76000	0.022
4	163900	0.038
5	365500	0.054
6	720100	0.072

Figure 6: Typical modeled causeway configuration including the selected locations for comparing lateral displacement results.

For getting converging solution, the causeway section used in the simulation was six meters thick which was a representative segment of a longer causeway. No movement was allowed for the base of the causeway in all directions while the ends and sides of the modelled

34

causeway were restricted from movement within their own plane. 3-D reduced intergration stress elements and nonlinear geometry were used. A surcharge load of 14 kPa was applied on the top of the causeway. This surcharge load was represented a two-lane road structure which was listed in Standard Specifications for Highway Bridges (AASHTO, [1]). In addition, three water depths (0.50, 1.50, and 2.50 m) measured from the causeway toe were considered during simulating the reference scenarios.

Five locations, as shown in Figure 6, on the causeway were chosen to compare the lateral displacement results between models without and with geotubes (scenarios shown later). These locations were located on the slip circle and were related to stability of slope.

2.1.3. Causeway designs with geotubes: Designed models

The following models aim to study the effect of different geometry of geotubes obtained from applying different pumping pressures p of 0.0, 5.0, and 20.0 kPa on causeways. These models were simulated without and with a surcharge load of 14 kPa and finally subjected to varying water depths (0.50, 1.50, and 2.50 m) due to the tidal effect. Geotextile tubes were used in order to improve the causeway slope stability by reducing the lateral displacement. The assumptions used when modelling the scenarios with geotubes were as follows:
1) The strength of geotextile material was higher than the stress caused by the applied loads.
2) The impact of geotextile seams and local imperfections on the geotube shape and strength were neglected during simulation.
3) Foundation soil had high bearing capacity.
4) The effect of sliding of the bottom tube was neglected.
5) The effect of scour was not under consideration.
6) Filling percentage of fill material was not under consideration in concluding the geometry of geotubes after filling procedure.

Again, it is worth mentioning that the geometry of the lower and upper tubes was obtained from the executed sub-models and the filling materials used during the designed models had the same characteristics of the causeway soil.

3. RESULTS AND DISCUSSION

3.1. Effect of geotube on the lateral displacement of the causeway at specific water depth and variable pumping pressures

Figures 7a and 7b showed the lateral displacement on the slope surface of the causeway without/with geotubes. They subjected to pumping pressure p = 0.0 and 5.0 kPa
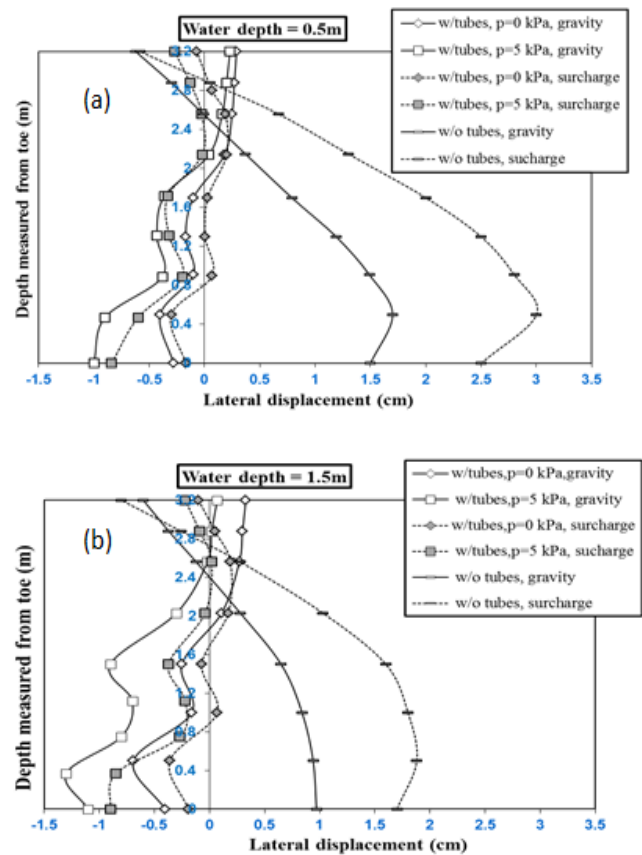

Figure 7: Lateral displacement for the causeway with geotubes with different pumping pressures: (a) at water depth = 0.50 m, and (b) at water depth = 1.50 m

even without/with surcharge load at water depths = 0.5 and 1.5 m measured from the causeway toe, respectively.

Due to the reduction in contact area between the upper and lower tubes as well in case of p = 20 kPa, the numerical solution was ceased which indicates to failure occurrence. The figures showed that, for both cases of loading, the geotubes significantly reduced the lateral displacement at the major vast locations on the causeway slope except at its upper part. Due to the absence of reinforcement by geotube at the top of slope, the lateral displacement values were higher in all cases of loading with geotubes subjected to p = 0.0 and 5.0 kPa with water depths = 0.50 and 1.50 m as compared to the case without geotubes. A third tube may enhance the lateral displacement behavior at the top of causeway slope. The figures also showed that the lateral displacement was lower in the case of p = 5.0 kPa as compared to p = 0.0 kPa. It seems that lateral displacement is decreased, especially at the toe, with increasing pumping pressure. However, as the current work considered only pumping pressures of 0.0, 5.0, and 20.0 kPa, future research should be oriented to investigate the effect of a wide range of pumping pressure on the lateral displacement. The decrease in lateral displacement with the increase of pumping pressure can be attributed to the changing of the tube geometry (height and

width). In other words, as the pumping pressure increased, the height of the tube increased and the width of the tube decreased. The figures displayed also that the lateral displacement values were higher when applying surcharge load than without in the case of causeway without geotubes. While with geotubes, the lateral displacement values were higher when applying surcharge load than without a surcharge load in the slope region reinforced by geotubes only. The figures revealed also that the differences in lateral displacement values on the causeway slope between the case of gravity load and when applying surcharge load were minimized when using geotubes. In addition, the location of the point of maximum lateral displacement value was also affected by the presence of geotubes. The maximum lateral displaced occurred at depth 0.45 m measured from the toe in the case of causeway without geotubes. However, two peaks of lateral displacement curves were observed when using geotubes caused maximum lateral displacement values to be located at depths 0.90 and 2.50 m measured from the toe at p = 0.0 and 5.0 kPa. By comparing the lateral displacement curves in figures 7a and 7b, it was noted that the difference in lateral displacement values between the case of gravity load and when applying surcharge load was less pronounced with water depth 0.50 m than 1.50 m. The differences in lateral displacement values under gravity load and when applying surcharge load are directly affected by the depth of water from the causeway toe.

Tables 3 and 4 showed the lateral displacement values at the selected locations for models of causeway loaded by surcharge load with/without geotubes under p = 0.0 and 5.0 kPa at a water depth equal to 0.5 m and 1.5 m measured from the toe, respectively. The most notable aspect in Tables 3 and 4 was that lateral displacement significantly reduced where the tubes were in place in all selected locations. The negative sign under (%) change refers that the deformation reduced in that particular value.

The maximum reduction in lateral displacement values was at the toe of causeway slope (location 3) with both water depths and under p = 0 and 5.0 kPa. On the other hand, lateral displacement at the top of the slope (location 1) was reversed to positive sign as shown in figures 7a and 7b. Once more, a third tube may correct the reverse lateral displacement behavior.

Table 3: Horizontal displacements at different locations in the causeway with surcharge load at pumping pressure of p = 0.0 and 5.0 kPa at water depth = 0.5 m.

Point	w/o tubes	U (cm) at P = 0.0 kPa		U (cm) at P = 5.0 kPa	
		w/ tubes	% +/-	w/ tubes	% +/-
1	+0.67	+0.189	-71.8	-0.02	-103
2	+2.30	+0.029	-98.7	-0.30	-113
3	+3.00	-0.310	-110.3	-0.60	-120
4	+3.36	+0.0095	-99.7	-0.01	-100
5	+3.18	+1.00	-68.5	-0.06	-102

Table 4, Horizontal displacements at different locations in the causeway with surcharge load at pumping pressure of 0.0 and 5.0 kPa at water depth = 1.5 m.

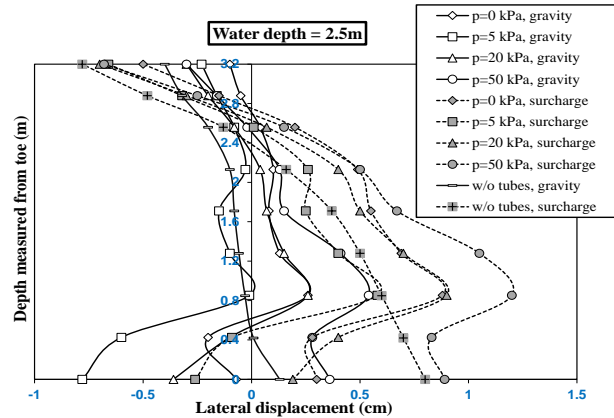| Point	w/o tubes	U (cm) at P = 0.0 kPa		U (cm) at P = 5.0 kPa	
		w/ tubes	% +/-	w/ tubes	% +/-
1	0.28	+0.18	-36	+0.02	-93
2	1.60	-0.07	-104	-0.30	-119
3	1.88	-0.30	-116	-0.80	-143
4	2.47	-0.10	-104	-0.20	-108
5	2.41	0.06	-98	-0.10	-104

Figure 8: Lateral displacement for the causeway with geotubes at water depth = 2.5m with different pumping pressures

Figure 8 showed the lateral displacement on the slope surface of the causeway without/with geotubes subjected to different pumping pressures for the case of water depth = 2.50 m. The results clarified that water depth had a great impact on the stability of geotubes, especially for the upper tube. High water depth increases the stability of geotubes at p = 20.0 kPa as it acts as an additional boundary condition that partially restrains the tube movement. The figure showed that the lateral displacement of the causeway slope was higher when applying surcharge load than without except at the upper part of the causeway slope. In addition, for both gravity load and when applying surcharge load, the using of geotubes with p = 0.0, 5.0, and 20.0 kPa significantly enhanced the lateral displacement at the toe of the causeway. However, the lateral displacement values were mostly higher in the other locations on the causeway slope when using geotubes with p = 0.0 and 20.0 kPa as compared to the case without geotubes. Only at p = 5.0 kPa, the lateral displacement values were lower than the case without geotubes in the slope region reinforced by geotubes. Also, the effect of geotubes on reducing the differences in lateral displacement between the gravity and surcharge cases of loading was unclear in the case of water depth = 2.50 m. As the water depth increased, the lateral water pressure on the geotubes increased, leading to more

Table 5: Horizontal displacements at different locations in the causeway with surcharge load at pumping pressure of 0.0, 5.0, and 20 kPa at water depth = 2.5 m.

Point	w/o tubes	U (cm) at P = 0.0 kPa		U (cm) at P = 5.0 kPa		U (cm) at P = 20.0 kPa	
		w/ tubes	% +/-	w/ tubes	% +/-	w/ tubes	% +/-
1	-0.13	+0.20	-254	+0.01	-108	+0.07	-154
2	+0.40	+0.50	25	+0.25	-38	+0.50	25
3	+0.75	+0.30	-60	-0.09	-112	+0.40	-47
4	+1.40	+0.90	-36	+0.80	-43	+1.10	-21
5	+1.20	+1.00	-17	+0.83	-31	+1.15	-4

lateral displacement for the causeway slope in case of using geotubes as compared to the case of without geotubes except at the toe of the causeway. For all pumping pressures, the point of maximum lateral displacement value was at the same depth which was 0.90 m above the slope toe.

Table 5 showed the magnitudes of the lateral displacement at the predetermined select locations (Figure 6) on the causeway without/with geotubes subjected to pumping pressures of 0.0, 5.0, and 20.0 kPa at water depth = 2.5m. Table 5 showed that maximum reduction in lateral displacement values in all selected locations was occurred at p = 5.0 kPa as compared to p = 0.0 and 20.0 kPa with the exception of location 1. It was noted that when using geotubes at water depth = 2.50 m the lateral displacement had opposing behavior as compared to the cases of water depths = 0.50 and 1.50 m. This can be attributed to the joint effect of high hydrostatic pressure and weight of the tubes. Based on the results shown in Figure 8 and Table 5, using of geotubes at water depth 2.50 m may not be the best solution to reduce the lateral displacement of the causeway if we considered its implementation cost.

3.2. Effect of geotube on the lateral displacement of the causeway at specific pumping pressure and variable water depths

As a desire to gather and compare the results of lateral displacement of the causeway at a specific value of pumping pressure under different water depths that someone may be interested to see, Figures 9a to 9c were presented. Figures 9a, 9b, and 9c showed the lateral displacement of the causeway subjected to different water depths for pumping pressures of 0.0, 5.0, and 20.0 kPa, respectively. Although these figures may be a repetition of the aforementioned results, we believe that these figures will provide more clarification for the obtained results and will help to draw solid conclusions. Furthermore, in order to save space and to avoid repetition, a brief narrative and explanation of the obtained findings from the shown figures were presented in the next few lines.

Figure 9a to 9c demonstrated that the magnitude of lateral displacement was considerably increased at the slope region reinforced by geotubes when applying surcharge load under all water depths. In addition, for all
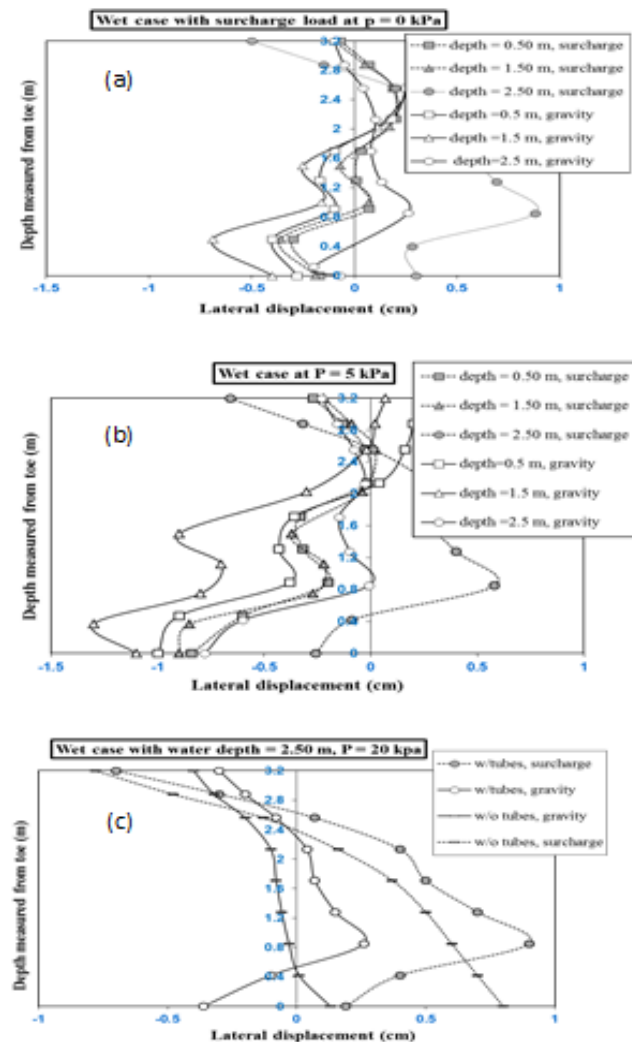

Figure 9: Lateral displacement for the causeway with different water depths; (a) pumping pressure = 0.0 kPa, (b) pumping pressure = 5.0 kPa, and (c) pumping pressure = 20.0 kPa.

water depths, the lateral displacement values were lower when using geotubes with p = 5.0 kPa than p = 0.0 kPa. Lateral displacements at water depth =1.5m was less than those at water depth = 0.5 at both of pressure = 0 and 5kPa. At water depth = 2.50 m, on the other hand, the geotubes did not show any significant effect on reducing lateral displacement, contrary, it increased the lateral displacement, except at the toe of the causeway, due to the effect of lateral water pressure on the geotubes and consequently on the slope of the causeway. Therefore, it is worth mentioning that the numerical solution under pumping pressure of 20.0 kPa was completed only with water depth = 2.50 m and the model results indicated that the geotubes in this case were useless with regard to reducing the lateral displacement.

In principle, using geotube with p = 5.0 kPa reduced the magnitude of lateral displacement more than p = 0.0 and 20.0 kPa with different water depths, specifically at water depths 0.50 and 1.50 m. Although, the stacked geotubes improved the lateral displacement behavior under water depths 0.50 and 1.50 m, some locations on the slope was bulged due to the transfer of geotubes own weight to the slope beneath.

4. CONCLUSION

Based on the aforementioned results, the following conclusion can be drawn:
• The ABAQUS model can be effectively used to get the deformed shape of any arrangement of geotubes subjected to different pumping pressures.
• Two stacked geotubes can develop an available and easy constructed pattern for the slope stabilization structure taking into account the pumping pressure forming the geotubes and water depth above the causeway toe.
• Applying surcharge load on the causeway increases the lateral displacement on the causeway slope even if geotubes were used.
• As the water depth increase to levels near the top of the causeway, the efficiency of geotubes in reducing lateral displacement diminish.
• Using geotubes configuration obtained from applying pumping pressure = 5.0 kPa is considered the most suitable option for reducing lateral displacement of the stuided causeway at lower water depths comparing to other tested pumping pressure.
• Variation of tidal range significantly affects the values of lateral deformation of the causeway at specific pumping pressure. As the water level exceeds a certain value, the magnitudes of lateral displacement increased.
• The ABAQUS model is not recommended for simulating causeway with geotubes formed from pumping pressure equal to or higher than 20.0 kPa combined with the lower water depth (0.50 and 1.50 m) due to the probable failure of the upper tube. The failure can be occurred due to a small contact area between the tubes and the slope and the absence of lateral restriction with lower water levels.

CREDIT AUTHORSHIP CONTRIBUTION STATEMENT:
Heba Koura: Literature review, Methodology, Software, Formal analysis, Original draft preparation; and Investigation; **Ehab Tolba:** Visualization, Conceptualization, Supervision, Investigation, and reviewing; **Elsayed Galal:** Visualization, Conceptualization, Methodology, Original draft preparation, Supervision, Editing, and Reviewing.

REFERENCES
[1] AASHTO. Standard Specifications for Highway Bridges, 17th Edition. Section 5.5.2, pg. 122.2002.
[2] CUR, "CUR 217: Ontwerpen met geotextiele zandelementen," Stichting CUR, Gouda, 2006.
[3] H.J. Kriel, "Hydraulic stability of multi-layered sand-filled geotextile tube breakwaters under wave attack," Master thesis, Civil Engineering Department, Faculty of Engineering, Stellenbosch University, South Africa, 2012.
[4] M.G. Latha, K. Rajagopal, and N.R. Krishnaswamy, "Experimental and theoretical investigations on geocell-supported embankments," Int. J. Geomech., vol. 1(30), pp. 30– 55, 2006.
[5] D. Leshchinsky, and O. Leshchinsky, "Geosynthetic Confined Pressurized Slurry (GeoCoPS): Supplimental Notes for Version 1.0," Report TR CPAR-GL-96-1, U.S. Army Corps of Engineers Waterways Experimental Station, Vicksburg, MS, 1996.
[6] G.S. Liu, "Design Criteria of Sand Sausages for Beach Defenses," International Association for Hydraulic Research: Summaries of Papers Proceedings, New Delhi, India, pp. 123-131, 1981.
[7] M.W. McElroy, "Three dimensional finite element modeling of stacked geotextile tubes for embankment stabilization," Master thesis, Civil and Environmental Engineering Department, Faculty of Engineering, Lehigh University, USA, 2008.
[8] P. Seay, "Finite Element Analysis of Geotextile Tubes," Virginia Technical Institute, 1998.
[9] S. Shoop, R. Affleck, V. Janoo, R. Haehnel, and B. Barrett, "Constitutive Model for a Thawing, Frost-Suseptible Sand," ERDC-CRREL TR-05-3, U.S. Army Cold Regions Research and Engineering Laboratory, Hanover, New Hampshire, 2005.
[10] C. Taechakumthorn, and R.K. Rowe, "Performance of reinforced embankments on rate-sensitive soils under working conditions considering effect of reinforcement viscosity," Int. J. Geomech., vol. 12(4), pp. 381–390, 2012.
[11] P. Vansteeg, and E. Vastenburg, "Large scale physical model tests on the stability of geotextile tubes," Deltares report, Delft, 2010.

[12] S.W. Yan, J. Chen, and L.Q. Sun, "Methods for designing partially inflated geotubes," Journal of Marine Science and Technology, vol. 24 (1), pp. 1-9, 2016.

[13] N.N.S. Yapage, D.S. Liyanapathirana, H.G. Poulos, R.B. Kelly, and C.J. Leo, "Numerical modeling of geotextile-reinforced embankments over deep cement mixed columns incorporating strain softening behavior of columns," Int. J. Geomech., vol. 15(2), 04014047, 2013.